*Polymer* Vol. 39 No. 23, pp. 5717–5724, 1998
0032-3861/98/$ – see front matter

PII: S0032-3861(97)10186-0

# The geometry of spherulite boundaries

**Z. H. Stachurski* and J. Macnicol**
*Department of Engineering, FEIT, The Australian National University, Canberra, Australia 0200*
*(Received 1 May 1997; revised 9 September 1997; accepted 24 September 1997)*

Spherulitic growth and the microstructure of crystalline polymers is proved to correspond to space filling by the expansion of spheres. Therefore spherulitic microstructures are analogous to space filled in by randomly nucleating (in space), expanding and touching spheres. This is contrasted with microstructures in metals, where surface tension leads to reshaping of the grain boundaries. Geometrical solutions are given for the general cases of grain-boundary surface shapes depending on the ratio of growth rates and contact radii. A space-filling computer model for expanding spheres is described, and the program's URL on the Internet is given. Several micrographs and figures are analysed to show the relationship between grain-boundary shapes and growth kinetics. Previous papers and computer models on this subject are reviewed. © 1998 Elsevier Science Ltd. All rights reserved.

**(Keywords: spherulites; boundary topology; growth kinetics)**

## INTRODUCTION

The morphology of grains and grain boundaries in polycrystalline metals has been much researched and described in published literature[1–4]. When referring to crystalline polymers, it is usually tacitly assumed that the microstructures observed are analogous to those observed in metals on the basis that spherulites are equivalent to grains[5]. Superficially (neglecting the fine structure within the spherulites) this appears to be so; the grain boundaries in polymers delineate shapes apparently similar to those found in single-phase metals. Furthermore, metallographic techniques developed for quantitative stereological measurements are applicable equally to both systems[6–8].

Following the work of Smith[1,2], it is now the generally accepted view that grain boundaries in metals change shape in the final stages of solidification (or during any subsequent heat treatment), and depart from the original topology of randomly distributed touching spheres. This grain regrowth occurs (by diffusion) to satisfy the condition of minimum surface energy and to equilibrate surface tension at boundary edges and corners; the latter requirement being responsible for the curving of the boundaries. The rate of adjustment, which is proportional to curvature, is greatest at grain corners, where one boundary meets other boundaries at nearly 120°. As a result, the original shape of the grains and their boundaries changes with time. This effect is illustrated in *Figure 1*, which shows four stages of grain-shape readjustment found in metals, reproduced from the original paper by Smith[1].

The main point intended by this preamble is that the shape of grain boundaries observed in metals is modified by grain regrowth, and therefore the observed microstructure does not represent the original random structure formed by nucleation, growth and impingement. The hypothesis is put forward here that in crystalline polymers regrowth of spherulites (and the accompanying shape change of boundaries) does not take place. Consequently the shapes of spherulite boundaries observed in polymers are those that formed as a result of random spatial distribution of nuclei, crystal growth and eventual meeting of the spherical growth surfaces on solidification. In that sense the shapes of grain boundaries in polymers are fundamentally different from those found in metals, which are modified by interfacial tension and diffusion. In this paper we elaborate on this unique relationship between the curvature of interspherulitic boundaries and growth rates of the adjoining spherulites.

The process of crystal aggregation into a spherulite is sensitive to external influences with the result that the spherical regularity is not always equally pronounced. Therefore it is necessary to assume that growth takes place under uniform fields of temperature and composition, so that the shape of the growing entity is solely a function of the intrinsic properties of the molecular or atomic constituents. Under these conditions, spherulites, as aggregates of single crystals radiating from the centre, will always assume the shape of a sphere, since the radial growth rate is the same in all directions. Adjacent spherulites, which possess spherical symmetry, always have the same crystallographic relationship to each other independent of their relative positions, and therefore the shape of the common boundary will be space-invariant. In metals, under the same conditions, the shape of a boundary between two growing metal grains should vary and be dependent on their relative crystallographic orientation[10]. However, in nearly isometric and pure metals (fcc, bcc) this effect is not pronounced, and grains grow as spheres to a good approximation.

From the above one can infer that microstructures found in crystalline polymers (formed on solidification under the specific conditions of uniform temperature and composition) are governed by the growth and impingement of perfectly spherical entities. It is convenient to describe the resulting shape of the spherulite boundaries by geometrical considerations of two expanding spheres that touch and grow to form a common boundary.

* To whom correspondence should be addressed

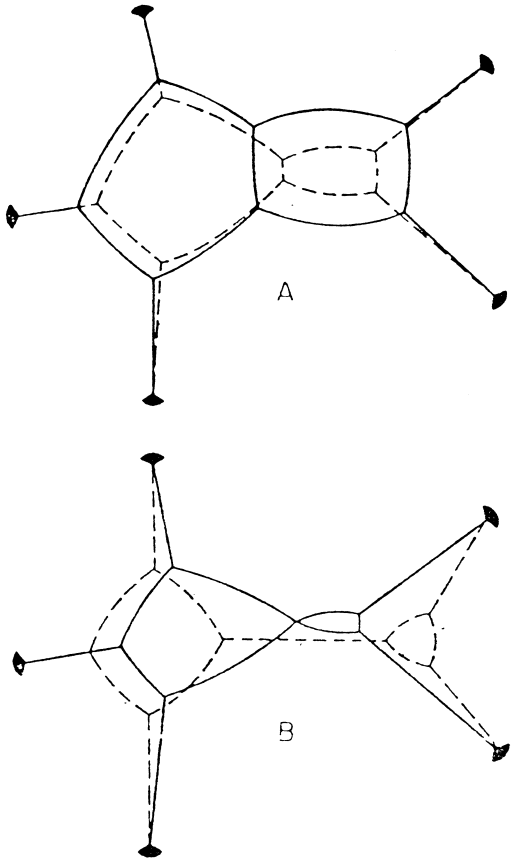


**Figure 1** Grain growth in metals. In A, the solid line shows the original grains surrounded by five adjacent grains (not shown in full); the broken line shows the change of grain boundary shape driven by surface tension and diffusion. In B, two further stages of grain growth are shown. Note the significant morphological changes between the original and final structures. At one stage four boundaries meet at one point—an energetically unfavourable configuration (reproduced from Ref. 1)

## GEOMETRICAL CONSIDERATIONS

Two points fixed in a Cartesian space are the centres of expanding (growing) spheres denoted as $\alpha$ and $\beta$; the radii of the spheres are $r_\alpha$ and $r_\beta$, respectively. At a time, $t = 0$, the spheres just touch, and we denote the magnitudes of the radii at that time as $r_\alpha = a$ and $r_\beta = b$. Let $G_\alpha$ and $G_\beta$ be the corresponding radial growth rates of the spheres so that, for times $t > 0$, the above quantities are simply related as follows: $r_\alpha = a + G_\alpha t$ and $r_\beta = b + G_\beta t$.

The spheres are not allowed to grow into each other, and when $(r_\alpha + r_\beta) > (a + b)$ the spheres form a common boundary. In general this is a three-dimensional surface possessing rotational symmetry around an axis formed by a line joining the centres of the spheres. Consider a cross-section through the spheres as shown in *Figure 2*. By Pythagoras' theorem: $AM^2 = AQ^2 + MQ^2$ and $BM^2 = MQ^2 + BQ^2$. Noting further that $AM = r_\alpha$, $BM = r_\beta$, $AQ = (a + b)/2 + x$, $BQ = (a + b)/2 - x$ and $MQ = y$, a general analytical expression of the common boundary surface can be derived in terms of the coordinates $x$, $y$ and $z$, and time $t$.

Restricting considerations to linear growth only (i.e. $G_\alpha$ and $G_\beta$ = constant) we find that there are four distinct shapes of the boundary arising. The parameters describing the four cases are summarised in *Table 1*, and are considered in more detail below.

*Case 1 (Table 1)*

In this case the growing spheres have the same radii at all times, and points $O$, $P$ and $Q$ coincide. The boundary between the two spheres is always planar in the form of a circle. The equations of the plane and of its diameter are:

$$x = 0 \tag{1}$$

$$d = \sqrt{(G_\alpha t + a)^2 - a^2}$$

The intersection of the spheres and their boundary with any plane $\pi$, randomly oriented in space, will result in two circular arches (from the spheres), attached to a common straight line (from the boundary). The intersection of the $\pi$ plane with the intersphere boundary is always a straight line.

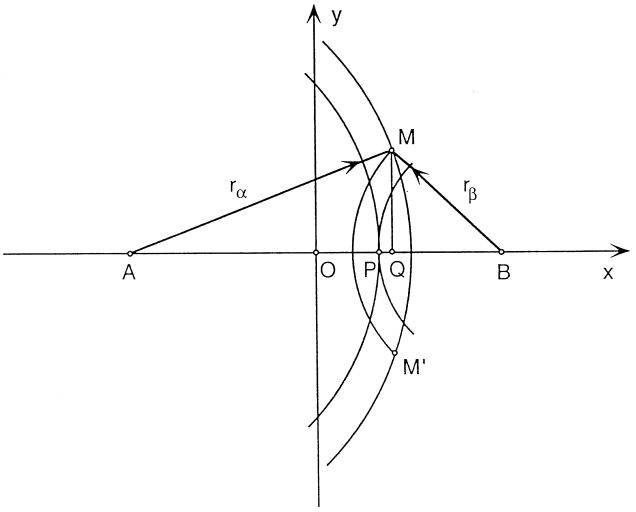


**Figure 2** Geometry of the cross-section through two expanding spheres, intersecting at a common boundary. Only small sections of the spheres are shown. The spheres initially touched at point $P$. At the first moment of touch the radii were $AP = a$, $BP = b$. Point $M$ is at the edge of the common boundary at a later time. The origin of the Cartesian axes is at $O$

*Case 2 (Table 1)*

In this case the spheres are always of different size, and the boundary is a curved surface. Its shape is given by the rotation of a hyperbola around a line joining the centres of the two spheres. In reference to *Figure 2*, with the origin of the $x$-axis at point $O$, the equation of the surface is:

$$\frac{(2x)^2}{(a-b)^2} - \frac{y^2 + z^2}{ab} = 1 \tag{2}$$

The surface is concave for the larger $\alpha$ sphere, and convex for the $\beta$ sphere. The intersection of any random plane $\pi$ with the boundary will always result in a hyperbola, providing the angle, $\lambda$, between the normal to the plane and the axis of rotation is greater than $\arctan[2\sqrt{ab}/(a-b)]$. For lesser angles the intersection will yield an oval, and finally a circle when the angle $\lambda = 0$ (here $a$ and $b$ are not the semi-axes of the hyperbola). Note that the shape of the boundary is independent of the magnitude of the growth rates. In semi-parametric form the equation of the hyperboloid surface is as follows:

$$x = \left(\frac{a-b}{2}\right) + G_\alpha \left(\frac{a-b}{a+b}\right) t \tag{2a}$$

$$z^2 = y^2 = (b + G_\alpha t)^2 - \left(\frac{a+b}{2} - x\right)^2$$

**Table 1** Four cases of boundary surfaces between growing spheres

| Case | Shape of boundary for $t > 0$ | Relationship between growth rates | Relationship between radii at $t = 0$ | Surface area of boundary at $t \to \infty$ |
|---|---|---|---|---|
| 1 | Flat plane | $G_\alpha/G_\beta = 1$ | $a = b$ | Unlimited |
| 2 | Hyperboloid | $G_\alpha/G_\beta = 1$ | $a > b$ | Unlimited |
| 3 | Sphere | $G_\alpha/G_\beta > 1$ | $a > b\ (G_\beta/G_\alpha)^a$ | Finite |
| 4 | Revolution of cardioid | $G_\alpha/G_\beta > 1$ | $a < b\ (G_\beta/G_\alpha)^a$ | Finite |

[a]These criteria are derived from the second term on the right-hand side of equation (3)

In the next two cases the $\alpha$ sphere is growing faster than the $\beta$ sphere. The one with the slower growth rate will always have a limited growth range because in due course, given sufficient time, it will be engulfed by the other sphere. However, the shape of the boundary surface will vary, depending on the relative size of the spheres when they touch, as expressed by the criteria in column 4, *Table 1*.

*Case 3 (Table 1)*

From the moment of touch, the slower growing $\beta$ sphere can only expand in directions away from the faster growing $\alpha$ sphere until a closure time, $t_c$, when the larger sphere completely encloses the smaller one. From then on, the $\beta$ sphere cannot grow any more and remains enclosed. The resulting common boundary is also a sphere. If the origin of the $x$-axis is taken as the point where the two spheres touched (point $P$ in *Figure 1*), then the equation of the boundary surface will be given by:

$$x = \frac{1}{2(a+b)}\left[\left(G_\alpha^2 - G_\beta^2\right)t^2 + 2\left(aG_\alpha - bG_\beta\right)t\right] \qquad (3)$$

$$z^2 = y^2 = \left(b + G_\beta t\right)^2 - (b - x)^2$$

If $G_\alpha = G_\beta$, and the origin is moved by the distance $(a - b)/2$ from $P$ to $O$, then equation (3) reduces to equation (2). In addition, if $a = b$, then equation (3) will reduce to equation (1). After an interval of time, given by $t_c = 2r_\beta/(G_\alpha - G_\beta)$, the form of equation (3) becomes closed and independent of time, reducing to:

$$\left(x - r_{\text{bound}}\right)^2 + y^2 + z^2 = \left(r_{\text{bound}}\right)^2 \qquad (3a)$$

where $r_{\text{bound}} = r_\beta(1 + \zeta)$, with $\zeta = G_\beta/(G_\alpha - G_\beta)$. The intersection of both $\alpha$ and $\beta$ spheres with any plane $\pi$, randomly oriented in space, will always result in two circles, one enclosed within the other. Notice that the diameter of the boundary is dependent on the growth rates through the parameter $\zeta$.

*Case 4 (Table 1)*

In this case the $\alpha$ sphere starts growing from a point on the surface of an already existing $\beta$ sphere, so that initially points $A$, $O$, $P$ and $Q$ coincide. At first the $\beta$ sphere will grow over the embryonic $\alpha$ sphere, confining the latter's growth in the negative $x$-axis direction. However, the faster growing $\alpha$ sphere will in time grow larger than the $\beta$ sphere and eventually engulf it and stop it from further growth.

The development of this boundary surface is also described by equations (3) and (3) with the origin of the $x$-axis at point $P$. The condition $a < b(G_\beta/G_\alpha)$ ensures that in equation (3) the second term for $x$ is negative, dominating the expression for small $t$. The initial growth in the negative $x$-axis direction will continue until a time $t' = (bG_\beta - aG_\alpha)/(G_\alpha^2 - G_\beta^2)$, as can be derived by differentiation with respect to $t$. The enclosure of the $\beta$ will take place at time $t_c$, given above for Case 3.

## COMPUTER MODELLING

We have developed a computer model to simulate the growth of spheres in space. The program is available as freeware on the Internet[11]. The processes of nucleation and growth are independent of each other, and are generated by appropriate algorithms. In this sense it is similar to models reported previously, which were developed to simulate single-crystal grain growth in metals and spherulitic growth in polymers[12–15]. However, there are several new features in our computer model which were not available previously.

First, the topology obtained is the result of a space-filling process, and not the result of analytical solutions as given above or in the previous computer models. The simulation is carried out in a virtual space represented in the computer by a lattice enclosed in a finite rectangular 'container'. Initially, all lattice points in the rectangular container are assigned as 'liquid' phase. Particles enlarge from the central nucleus in proportion to the growth rate, which may vary in space. Lattice points within each particle are identified as 'solid' phase, and lattice points separating the two phases are assigned as 'boundary'. When two particles meet, a common boundary is also established by a simple algorithm identifying the values of neighbouring lattice points. The display of the microstructure is obtained by executing a plane 'cut' through the container, and the visualisation is achieved by assigning different values to (1) liquid pixels (white), (2) solid pixels (grey or colour) and (3) boundary pixels (black), which correspond to the appropriate lattice points. By executing one-by-one plane cuts, a tomography of the microstructure can be obtained.

Second, the model has the ability to nucleate and grow two (or more) species independently. This is for the case of nucleation from the liquid phase only, and it correspond to the solidification of a binary immiscible mixture. At this stage variations in liquid composition are not taken into account.

Third, the space-filling method allows for an easy implementation of temperature, density and composition gradients. Analytical solutions involving all three effects are difficult to implement; by contrast, this method lends itself naturally to implementation of externally imposed fields considered on a local scale of neighbouring cells at a time.

The model obeys the law of conservation of mass:

$$X_S + X_L + X_b = 1 \qquad (4)$$

$$\frac{dX_S}{dt} = -\frac{dX_L}{dt} \qquad (5)$$

where $X_S$, $X_L$ and $X_b$ are the mass fractions of the growing

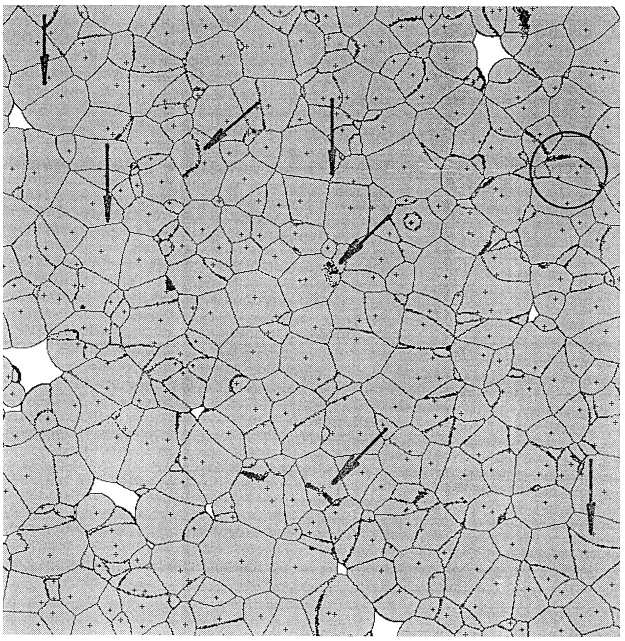

**Figure 3** Spherulite microstructure corresponding to Case 2 (and occassionally Case 1) obtained from the computer model described in the text. The small crosses indicate projections of the spherulite centres onto the plane of view. Note: (1) two straight boundaries pointed out by down arrows on the left-hand side; (2) hyperbolic boundaries (some pointed to by arrows); and (3) one near-circular feature formed by 'grain capping'. Other features are described in the text

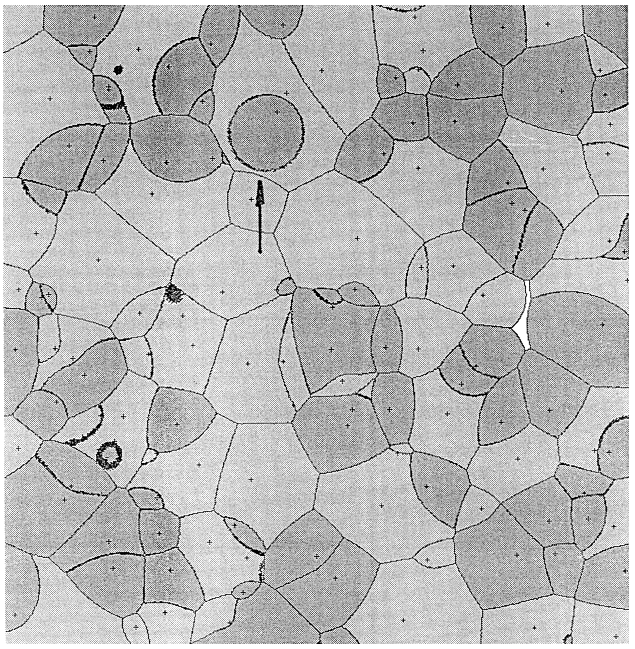

**Figure 4** Microstructure of two types of spherulite, corresponding to Case 3, obtained from the computer model described in the text. The small crosses indicate projections of the spherulite centres onto the plane of view. All boundaries between spherulites of the same type are hyperbolic, all boundaries between differing spherulites are circular. Note especially the circular boundary pointed to by the arrow

spheres and liquid, and that of the boundary, respectively. Since $X_b \ll X_S$ or $X_L$, the error in equation (5) due to omission of the boundary is small. Since we assume the density of all the phases to be the same and equal to 1, the model therefore obeys the law of conservation of volume; i.e. volume fractions and mass fractions are equivalent at all times[16].

*Figure 3* shows the microstructure obtained from one of the simulations on a single species for thermally activated nucleation, and illustrates both Cases 1 and 2 described above. The simulation was carried out in a container comprising $675 \times 675 \times 90$ lattice points. The depth of the container is chosen to be approximately twice the diameter of the largest spherulite that can be expected for the given species and temperature. The cross-section shown is at approximately 3/4 of the depth, chosen specifically to illustrate some of the salient features predicted by the model and to be representative of the entire structure (not affected by the presence of the walls of the container). Most grain boundaries are essentially a single pixel wide; these are making a large angle with the plane of the cross-section (plane of the picture). Some boundaries are, however, smeared (three examples are pointed to with slanting arrows), which indicates a small, grazing angle between the boundary surface and the cutting plane, and the fuzziness appears because of the fact that boundary pixels occupy finite volume as previously explained.

The small crosses indicate projections of the centres of each spherulite onto the plane of the cross-section. In the encircled area the spherulite denoted as 1 contains three crosses. The middle cross identifies the centre of this spherulite, the one above and slightly to the right identifies the centre of spherulite 2, and the third cross to the left and slightly down identifies the centre of spherulite 3.

Straight boundaries appear between spherulites of which the centres are equidistant from the boundary, i.e. that nucleate at the same time. Hyperbolic boundaries occur between spherulites that were nucleated at different times. Four boundaries meeting at one point also appear, as well as a circular boundary wholly within another spherulite. These features are indicated in the figure by the down-pointing arrows.

Novel microstructures are generated when spheres of a different type are allowed to grow within the volume of the matrix. *Figure 4* shows a two-phase microstructure generated by our computer model, consisting of $\alpha$ and $\beta$ spheres treated as distinct phases with different nucleation and growth kinetics. Two features are noteworthy: (1) spherical $\beta$ particles are formed within the faster growing $\alpha$ phase as predicted by Case 3 above; and (2) clustering of $\beta$ cells which were not incorporated into the $\alpha$ cells but grew to form separate spherulites. Finally, *Figure 5* shows the cross-section of the cardioid-like shape generated in accordance with Case 4 above. In principle such shapes could form during simulations similar to that shown in *Figure 4*, but are unlikely to be found frequently owing to their low probability of occurrence.

## SPHERULITE MICROSTRUCTURES IN POLYMERS

Published literature contains numerous examples of micrographs of spherulites in polymers, illustrating most of the geometrical shapes described above. The first classic example, shown in *Figure 6*, is that of spherulites grown in a thin film of isotactic polystyrene from the work of Keith[17]. The two selected spherulites, marked $\alpha$ and $\beta$, are very closely of the same size and are assumed to have grown at the same rate. The boundary between them is a straight line as predicted by Case 1. Examples of such straight boundaries are abundant in the published literature on polymers.

The next example, from an early work of Keller[18], is that

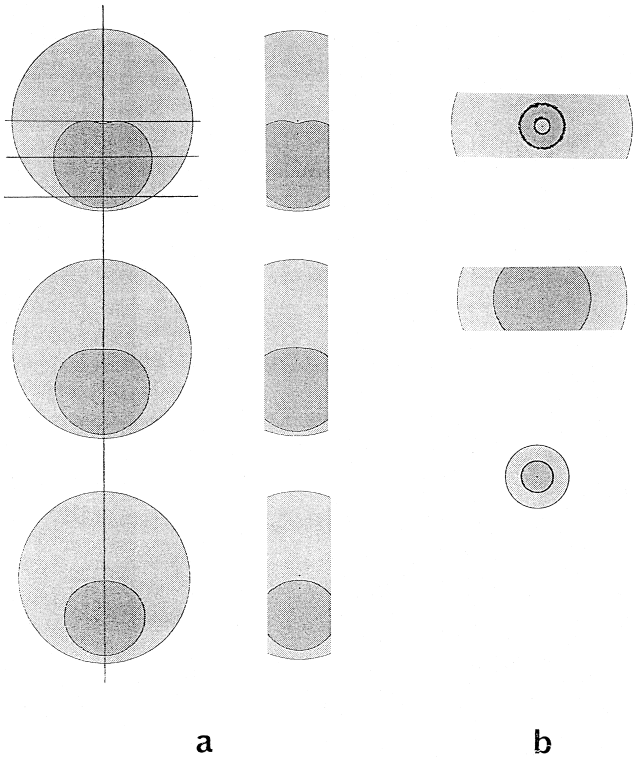


**Figure 5** The shape of interspherulite boundary corresponding to Case 4 in *Table 1*. (a) The *xz* and *yz* cross-sections, obtained at different depths; (b) the *xy* cross-sections, indicated in the top left picture by the three horizontal lines. These diagrams prove the cardioid-like shape of the interspherulite boundary

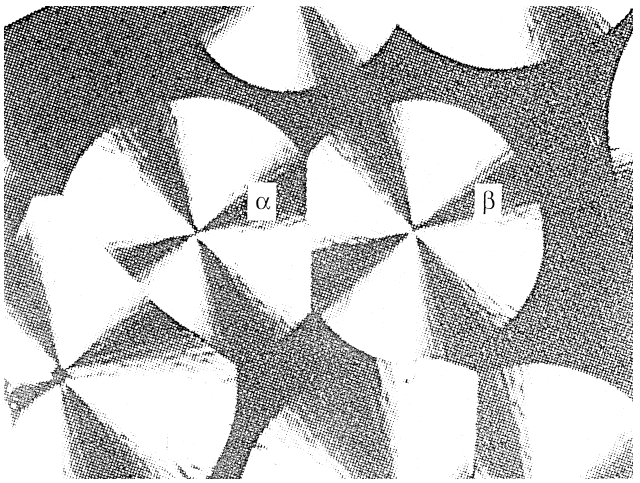


**Figure 6** Two spherulites, of the same radius and growing at the same rate, produce a straight-line common boundary in accordance with Case 1 for an $\alpha$ and $\beta$ sphere (micrograph reproduced from Ref. 17)

of banded spherulites grown in a thin film of poly(trimethylene glutarate), as shown in *Figure 7*. The equally spaced rings, formed by twisting fibrils within the spherulite, provide evidence that a constant growth rate prevailed for both the $\alpha$ and $\beta$ spherulites[19]. Note that, on touching, the radius of the $\alpha$ spherulite was larger than the radius of the $\beta$ spherulite ($a > b$). The spherulites grew to form a hyperbolic boundary as predicted by Case 2. The centres of the spherulites are in the plane of the micrograph, therefore the radii of the spherulites can be measured off the picture. From the properties of hyperbolae one finds that the asymptotes are inclined to the *x*-axis with a gradient given

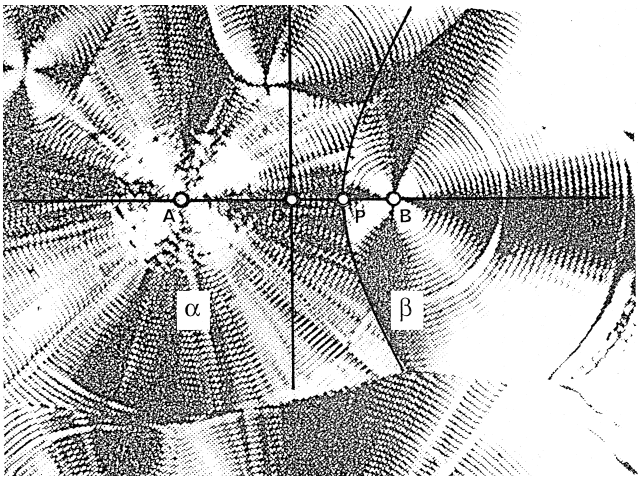


**Figure 7** Two spherulites, growing at the same rate, but nucleating at different times ($a > b$), result in a hyperbolic boundary in accordance with Case 2 for an $\alpha$ and $\beta$ sphere (micrograph reproduced from Ref. 18)

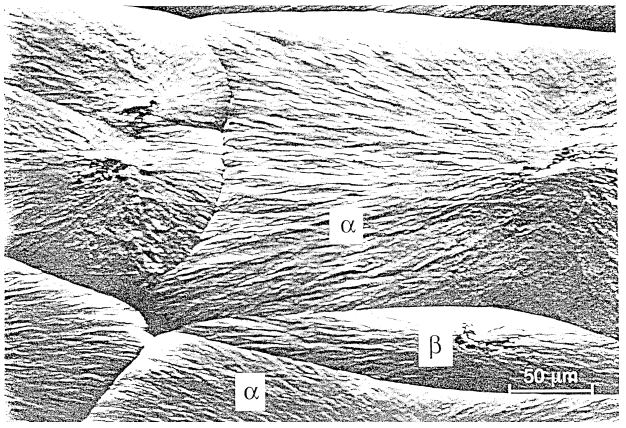


**Figure 8** Hyperbolic boundaries between spherulites as viewed by scanning electron microscopy (micrograph reproduced from Ref. 20)

by $2\sqrt{ab}/(a-b)$. The construction lines and the hyperbola were drawn onto the micrograph to show how good the agreement is between the geometrical predictions and the observed shape. To further illustrate the hyperbolic curvature of interspherulite boundaries, we examine the micrograph in *Figure 8* showing a cross-section through three spherulites[20]. Although the conditions of growth are unknown in this case, we may speculate that they approximated constant and uniform growth rate. The interpretation of the observed microstructure would be that the in-between spherulite has a smaller radius than the two adjacent ones, and that (1) the centres of the spherulites are coplanar or (2) its centre is below the plane of the centres of the other spherulites. The cut through the grain boundaries forms a lens-like shape because it corresponds to two images of Case 2.

One further example of the hyperboloid boundary between spherulites is shown in *Figure 9*, taken from Ref. 21. The interesting point to note is that these are observed in a metallic system, and therefore provide evidence for the assertion that the shape of interspherulitic boundaries is governed by geometrical considerations and is independent of the chemical nature of the substance.

For the next case we present the micrograph in *Figure 10* from Ref. 22 of spherical particles appearing within larger spherulites in a binary immiscible mixture of polyethylene

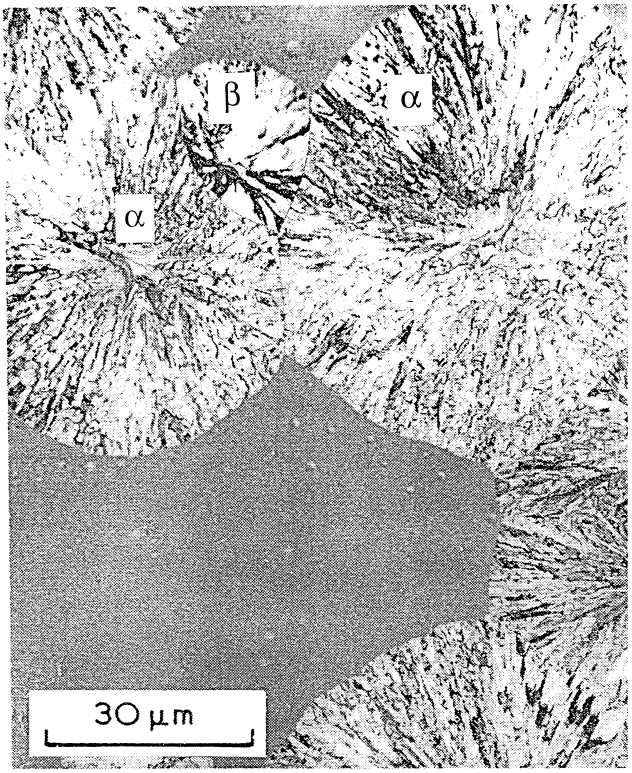


**Figure 9** Hyperbolic boundaries between spherulites in a metallic alloy (micrograph reproduced from Ref. 21)

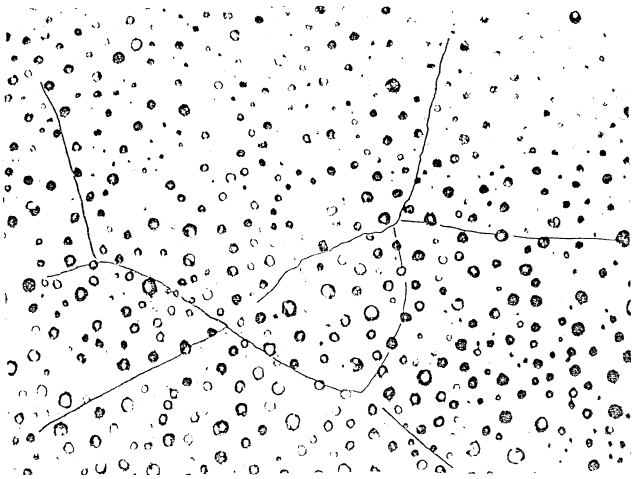

**Figure 10** Spherical polyethylene particles within polypropylene spherulites. It is assumed that the polypropylene spherulites crystallised at a faster rate than polyethylene, thus engulfing and enclosing the small polyethylene spherulites in accordance with Case 3 (micrograph reproduced from Ref. 22)

and polypropylene, which purports to illustrate Case 3. Here we find small, round crystalline polyethylene phase, enclosed within the large polypropylene spherulites. It is reasonable to assume that polypropylene crystallised at a faster rate than polyethylene, engulfing it during growth. However, it is uncertain whether this microstructure formed necessarily by the mechanism identical with Case 3. It is possible, for example, that molten polyethylene phase was entrapped within the polypropylene spherulite, and that it solidified at a later stage. No further direct examples of Case 3, conforming strictly to the conditions of constant temperature growth, are known to the authors.

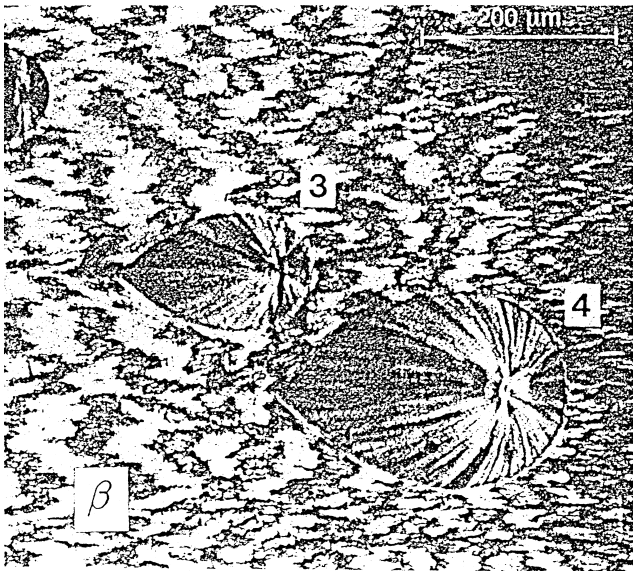


**Figure 11** An unusual shape of spherulites within another crystalline phase. This micrograph shows a stage during directional solidification of a thin film of isotactic polypropylene. The crystalline phase, horizontally oriented, can be considered as a large spherulite within which small spherulites of a different phase nucleated and grew. This possibly illustrates Case 3 but for the situation in which the ratio $G_\alpha/G_\beta$ is not constant during growth (micrograph reproduced from Ref. 23)

Finally we note another intriguing micrograph, reproduced here from a paper by Lovinger[23], and shown in *Figure 11*. This is another example of the $\alpha/\beta$ growth of spheres with unequal growth rates. The unidirectional matrix, showing preferred orientation in the horizontal direction, is the crystalline phase of polypropylene (Type IV crystal structure). It can be considered as a segment of a spherulite of infinitely large radius. Within the matrix appear other spherulites with teardrop-like shape (Type I crystal structure). Initially (before doing the mathematics) we thought this shape to result from growth in accordance with Case 3. However, according to the authors, this is due to the conditions of growth departing from the quiescent state, and experiencing a temperature gradient.

## DISCUSSION

The specific Gibbs free energy of grain boundaries in metals is substantially higher than its value within the body of the grain. This provides the necessary driving force for the minimisation of grain-boundary surface area. In polymers, due to the complex internal microstructure of the spherulite, the specific Gibbs free energy associated with the interior of the spherulite is not less, and can be greater, than that associated with the interspherulitic boundary. Therefore the important observations can be made that: (1) there is no driving force (or it is too small) to change the shape of interspherulite boundaries and, as a consequence, (2) there is a unique relationship between the curvature and shapes of the interspherulitic boundaries and the growth rates of adjacent spherulites. In particular, this relationship holds information about the kinetics of crystallisation, and can be used to advantage when other evidence is not available.

For example, the hyperbolic grain boundary shape always implies Case 2 growth kinetics. In a paper on spherulitic morphology of isotactic polypropylene[24], Norton and Keller include a micrograph (Figure 1c) showing one spherulite with the so-called Type I crystal structure, surrounded by

other spherulites of the Type IV crystal structure, grown isothermally at 125°C. Those authors, referring to a previous publication[23], assert that the Type IV spherulites must have grown at a higher rate than the Type I spherulite. However, it can be observed that the shape of the boundaries with the adjacent spherulites is hyperbolic, which, by the observations above, implies unequivocally that both types of spherulite had exactly the same growth rate, contrary to the statements by the previous authors.

If the nucleation of all spheres of one type is instantaneous, the computer model generates constructions in accordance with Case 1 above, and simulates polymer microstructures identical to those described by Mahin *et al.*[12] and Saetre *et al.*[14] as site saturation, and by Galenski and Piorkowska[15] as athermal nucleation. The microstructures generated show intercellular boundaries as straight lines. From the mathematical point of view this is equivalent to Dirichlet partition of a plane in two dimensions[25], and to Voronoi tessellation of space in three dimensions[26].

If the nucleation is sporadic (and all spheres of the same type), then the computer model generates growth in accordance with Case 2 above, and that described by Mahin *et al.*[12] and Saetre *et al.*[14] as Johnson–Mehl kinetics, and by Galenski and Piorkowska[15] as thermal nucleation. In two dimensions this results in hyperbolic boundaries—a fact recognised by Mahin *et al.*[12] (see their Figure 3), and also shown clearly in Figure 4 of Ref. 15.

Circular or oval inclusions of one phase within another are predicted by both Case 2 and Cases 3 and 4. The appearance of particles relating to Case 3 is shown for a real polymer in *Figure 10*, and for computer simulation in *Figure 4*, and has been explained as the result of the faster growing phase enveloping another slower growing phase. However, such 'inclusions' can also occur in single-phase crystallisation in accordance with Case 2 as already alluded to in preceding paragraphs. A plane of cross-section, passing through the hyperboloid boundary inclined at an angle $\lambda = 0$, will result in a circular trace. This effect has been observed by Mahin *et al.*[12], who referred to this as 'grain capping' (their Figure 4), also by Saetre *et al.*[14] in their Figure 1b, and in our computer-simulated microstructures, as shown in *Figure 3*.

The assumption of homogeneous temperature requires that the temperature is the same everywhere, ensuring that spherulites of the same type grow at the same rate. However, in single-phase systems, under continuous cooling conditions the rate of growth of the spherulite will vary, but the variation will be the same for all spherulites (i.e. $G_\alpha/G_\beta =$ constant). Therefore the geometry of the interspherulite boundaries will be the same as in an isothermal case. In multiphase systems, with different melting points and glass transition temperatures, the ratio $G_\alpha/G_\beta$ will not be constant during temperature variation, and may change from being greater than unity to less than unity during the cooling cycle. It is easily appreciated that, with such changes, the geometry of the interspherulite boundaries will be far more complex than that described by Cases 3 and 4 above. We suspect that this situation arose during the directionally solidified polypropylene, shown here in *Figure 11*, resulting in the drop-like shape instead of circular.

Recrystallisation of another kind does occur in polymers; the increasing degree of crystallinity with time in polyethylene[27] is attributed to secondary crystallisation. Secondary crystallisation involves sideways growth of lamellae within the uncrystallised regions of the spherulite or lamellar thickening[28]. It is well established that this continuing crystal growth is happening within the spherulites, whose boundaries are fully formed, and which do not change shape as a result of this process. Another occurrence of increasing degree of crystallinity with time is found in some glassy polymers, such as poly(ethylene terephthalate), due to actual growth of the crystalline phase at a very low rate owing to high viscosity of the matrix. Therefore the shape of the boundaries and the resulting microstructure, as a general rule, should not change on cooling or annealing.

The separation and formation of phases in immiscible mixtures occurs differently in metals and polymers. In metals, the microstructure is determined by the shape of primary grains formed on solidification, and by the shape of secondary grains (precipitates) formed during cooling from high temperature or on subsequent annealing. In polymers, solid/solid transformations which lead to the formation of new phases, such as precipitation from solid solutions, are not commonly observed. Therefore microstructures observed in solid polymers are those formed during the liquid-to-solid transformations mainly. Microstructures of the type shown in *Figure 4* are not seen in polymers, but they appear frequently in low-molecular-weight substances.

In metals, as a consequence of grain regrowth after solidification, the grain count will always underestimate the number of nuclei. Furthermore, it was shown that continuous grain growth in $\alpha$-brass not only leads to grain shape changes, but also results in significant texture changes[29]. This means that corners formed by four adjacent grains (formed by chance during solidification) should be observed in real polymer microstructures, but should never be seen in metal microstructures. An example in polymers of four boundaries meeting at one point is given in Ref. 24 (Figure 1a). Many other examples can be found in the literature. Our computer model also predicts this structure (see *Figure 3*).

In conclusion, it is emphasised that the ratios of $G_\alpha/G_\beta$ and $a/b$ of two adjacent spherulites play paramount roles in the shape of the grain boundaries, and hence that of the final microstructure.

## ACKNOWLEDGEMENTS

One of us (JM) acknowledges the assistance received from the ARC Grant No. SARC94030, entitled 'Kinetics of Microstructure Development in Modified Epoxy Resins', during programming of the spherulite growth model.

## REFERENCES

1. Smith, C. S., in *Metal Interfaces*. Am. Soc. for Metals, Cleveland, OH, 1951, p. 65.
2. Smith, C. S., *Metall. Rev.*, 1964, **9**(33).
3. Chalmers, B., *Principles of Solidification*. R. E. Krieger Publishing Co., Malabar, FL, 1982.
4. Mills, K. (Ed.), *ASM Handbook: Metallography and Microstructures*. Vol. 9. ASM International, New York, 1995.
5. Woodward, A. E., *Atlas of Polymer Morphology*. Hanser Publishers, Munich, 1989.
6. DeHoff, R. T. and Rhines, F. N., *Quantitative Microscopy*. Tech-Books, Hemdon, VA, 1968.
7. Vander Voort, G. F., *Metallography, Principles and Practice*. McGraw Hill, Inc., New York, 1984.
8. Russ, J. C., *Computer Assisted Microscopy*. Plenum Press, New York, 1991.
9. Mullins, W. W., *MRS Bull.*, July 1996, p. 24.
10. Mullins, W. W., *J. Appl. Phys.*, 1956, **27**, 900.
11. Mcnicol, J. and Stachurski, Z. H., *UVIRA: Simulation of Spherulitic Solidification in Polymers*. ANU, Canberra, Australia, 1997. http://spigot.anu.edu.au/people/zbigniew/uvira.html.

12. Mahin, K. W., Hanson, K. and Morris, J. W. Jr., *Acta Metall.*, 1980, **28**, 443.
13. Hanada, S., Ogura, T., Watanabe, S., Izumi, O. and Masumoto, T., *Acta Metall.*, 1986, **34**(1), 13.
14. Saetre, T. O., Hunderi, O. and Nes, E., *Acta Metall.*, 1986, **34**(6), 981.
15. Galenski, A. and Piorkowska, E., *Colloid Polym. Sci.*, 1983, **261**, 1.
16. Long, Y., Shanks, R. A. and Stachurski, Z. H., *Prog. Polym. Sci.*, 1995, **20**, 651.
17. Keith, H. D., in *Physics and Chemistry of the Organic Solid State*, eds D. Fox, M. Labes and A. Weissberger. Wiley Interscience, New York, 1963.
18. Keller, A., *J. Polym. Sci.*, 1959, **39**, 151.
19. Keller, A., *J. Polym. Sci.*, 1955, **XVII**, 291.
20. Martuscelli, E., Silvestri, C., Addonizio, M. L. and Amelino, L., *Makromol. Chem*, 1986, **187**, 1557.
21. Cantor, B. and Cahn, R. W., *J. Mater. Sci.*, 1976, **11**, 1066.
22. Stachurski, Z. H., Edward, G. H., Yin, M. and Long, Y., *Macromolecules*, 1996, **29**, 2131.
23. Lovinger, A. J., Chua, J. O. and Gryte, C. C., *J. Polym. Sci., Polym. Phys.*, 1977, **15**, 641.
24. Norton, D. R. and Keller, A., *Polymer*, 1985, **26**, 704.
25. Gersho, A., *IEEE Trans. Inform. Theory*, 1979, **IT-25**, 373.
26. Voronoi, G., *Journal für die reine und angewandte Mathematik*, 1908, **198**, 134.
27. Sharples, A., *Introduction to Polymer Crystallisation*, London, E. Arnold, 1966.
28. Bassett, D. C., *Principles of Polymer Morphology*, Cambridge Solid State Science Series, Cambridge University Press, Cambridge, 1981.
29. Abrruzzese, G. and Lücke, K., *Acta Metall.*, 1986, **34**, 905.